Unravelling glycosylation reaction mechanisms

Vrande, K.N.A. van de

Chapter 1: General Introduction and Outline

The group of biomolecules known as carbohydrates contains some of the most functionally and structurally diverse molecules.[1] With functions ranging from cell recognition[2] to immune response[3] and energy storage,[4] carbohydrates receive significant interest both in medical applications[5–7] and chemical and biological studies.[8] Investigating which function a specific carbohydrate fulfils can be done by using chemically synthesised fragments, which can serve as well-defined model compounds. However, the synthesis of carbohydrate fragments is not straightforward. When, during the synthesis of a certain carbohydrate fragment, a new glycosidic bond is formed, two possible diastereomers (anomers) can be formed: the α and β anomers (Figure 1). The anomers are labelled relative to the highest-numbered asymmetric carbon (reference atom).[9] If in the Fisher projection, the anomeric group is on the same side of the ring as the reference atom, this is called α, if the anomeric group is on the opposite side as the reference atom it is called β. Instead of the α- and β-designation, *cis*/*trans* nomenclature can also be used to differentiate between the anomers. This nomenclature denotes the orientation of the glycosidic linkage, relative to the functional group at C-2.

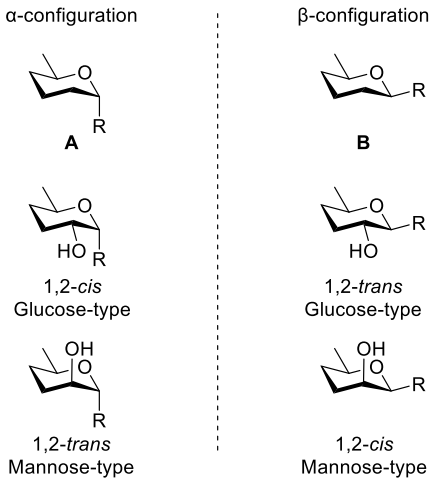

Figure 1: Generic structure of a carbohydrate in the α (A) and β (B) configuration.

The main issue in chemical glycosylation reactions is that it is not always straightforward to obtain the desired anomer in good selectivity. Generally speaking, 1,2-*trans* glycosidic bonds are relatively easy to synthesise, since neighbouring group participation can be used to steer the reaction towards the desired outcome.[10] For *cis* glycosidic bonds, on the other hand, no general methodology is available.[11–13] Because the mechanism of the reaction is complicated, the stereochemical outcome of a glycosylation reaction cannot be easily controlled.[14] Instead of going via a well-defined S_N1 or S_N2 mechanism, the glycosylation reaction exists on a spectrum in between these two mechanisms and has characteristics of

both.[14,15] The reaction mechanism spectrum is depicted in Figure 2. Upon activation of a carbohydrate donor, several reactive intermediates can be formed. As most activators used to date, employ triflate-based electrophiles, the spectrum shows a triflate as a leaving group/counterion. On either end of the spectrum, an anomeric triflate can be found, having either α- or β-configuration. This covalent intermediate reacts via an S_N2-like mechanism. In the centre of Figure 2, the solvent-separated ion pairs (SSIPs) are shown, which react via an S_N1-like mechanism. In between the covalent species and the SSIPs, the contact ion pairs (CIPs) are found. For these systems, the covalent bond between the carbohydrate fragment and the triflate is broken, but the two fragments are still close together, and the position of the triflate can influence the stereochemical outcome of the reaction. Where exactly on this spectrum a given glycosylation reaction will take place depends on several factors, including the polarity and nature of the solvent,[16] the reaction temperature,[17] the reactivity of the donor [18,19] as well as the reactivity of the acceptor. [20,21] This intricate combination of factors complicates investigating the mechanism of the glycosylation reaction. In this thesis, isotope labelling is used to shine more light on the mechanisms of these reactions. There are several ways in which the enrichment of a molecule with heavy isotopes can be used to gain insight into its reactivity. This ranges from relatively straightforward techniques, for example using NMR to find out where a certain atom in the starting material ends up in the final product, to more complex techniques, such as the establishment of Kinetic Isotope Effects (KIEs).

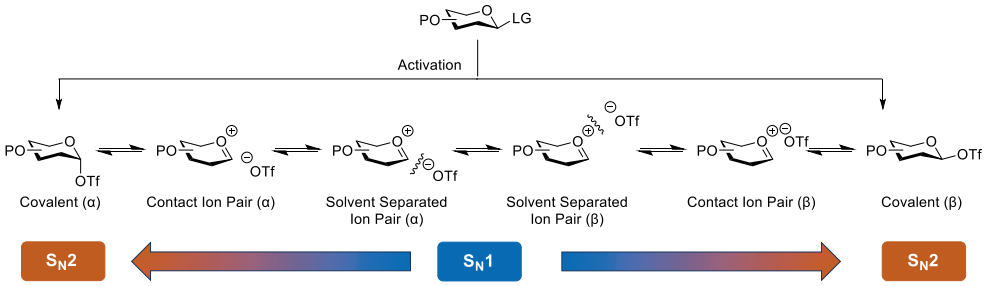

Figure 2: Spectrum of the reactive intermediates and mechanisms of the glycosylation reaction.

NMR Active Isotope Labelling

The easiest use of isotopic labelling to unravel molecular structures and reaction mechanisms is by labelling the starting materials with NMR active isotopes.[22] This way, a certain signal in the NMR can be amplified, for example, by exchanging an NMR-silent ^{12}C with the NMR-active ^{13}C isotope, or decreased, by for example substituting a proton (^{1}H) with deuterium (D, ^{2}H). This not only affects the NMR signal of the specific atom being exchanged but also the *J* coupling of the neighbouring atoms will be affected, providing information on these atoms as well.[23] An example is shown in Figure 3A, which depicts a study by Hamagami *et al.,* who determined the conformation of the tri- and tetrasaccharide **1**.[24] In this structure, the middle (purple) monosaccharide was fully labelled with both ^{13}C and ^{2}H labels. This allowed for the ^{3}J coupling constants between the carbon atoms in the central, labelled sugar and the carbon atoms at the other sides of the glycosidic bonds to be

determined. Since the $^{3}J_{C,C}$ coupling constant is related to the dihedral C-O-C angle via the Karplus equation, this allowed Hamagami *et al.* to determine the dihedral angles of the glycosidic bonds in **1**.[24,25] Isotope labelling in combination with NMR spectroscopy can also be used to elucidate the mechanism of a certain reaction, as was done by Dessinges *et al*. (see Figure 3B).[26] When treating glucoside **2** with sodium azide, the norbornane-like galactose **3** is formed. Two possible mechanisms can account for the formation of this product: either a ring contraction can give intermediate **4**, followed by an attack of the anomeric oxygen atom, liberated by nucleophilic attack of the azide at the anomeric ester, on position 5, or via the boat-like intermediate **5**, where the anomeric oxygen attacks position 4. Dessinges *et al.* labelled the anomeric oxygen with an ^{18}O isotope. Although ^{18}O is not NMR active, labelling a compound with ^{18}O does have an effect on the chemical shifts of the attached ^{13}C NMR peaks.[27] Using this method, it was found that the NMR signals of C-4 in the product were shifted compared to the natural ^{16}O containing compound, leading to the conclusion that the mechanism proceeds via intermediate **5**.

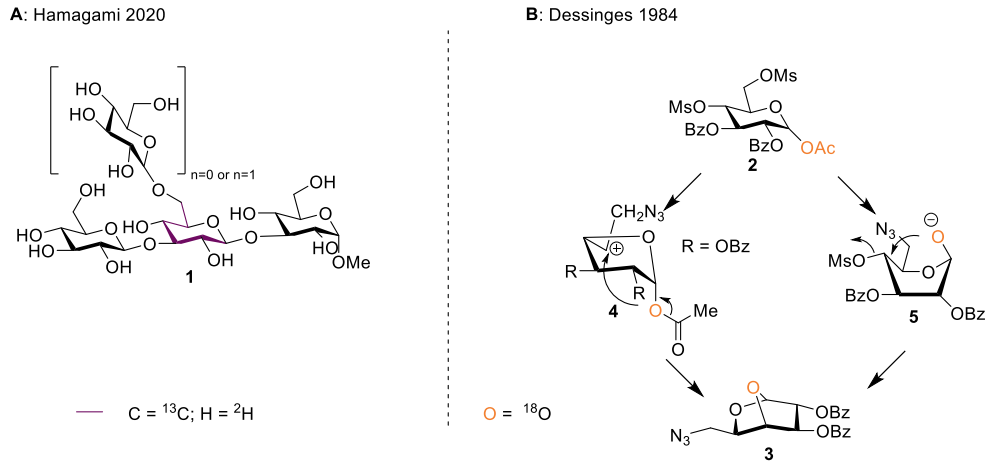

Figure 3: (A) Use of a fully ^{13}C and ^{2}H fragment in an oligosaccharide to determine the bond angles with NMR.[24] (B) Use of ^{18}O labelling to determine the reaction mechanism.[26]

The previous examples show how a combination of isotopic labelling and NMR spectroscopy can be used to investigate chemical structures and reaction mechanisms by measuring the spectrum of a stable product. Using more advanced NMR techniques, transiently formed intermediate structures can also be detected, as was done by de Kleijne *et al.* (see Figure 4).[28] They investigated the species formed upon activation of mannosyl donor **6**. After activating the donor with Ph_2SO and Tf_2O, two intermediates are formed: the dioxanium ion **7**, an intermediate yielding the α-product, and α-triflate **8**, which is involved in an S_N2 reaction leading to the β-product. Of these two intermediates, only **8** can be observed using standard NMR procedures, even when ^{13}C labelling is used. By using Chemical Exchange Saturation Transfer (CEST) NMR, the equilibrium between **7** and **8** can be utilized to indirectly visualise **7**. In CEST NMR, a range of NMR frequencies is scanned and saturated. Due to the

equilibrium between observable (**8**) and unobservable (**7**) intermediates, the scanning of the frequency of the invisible component will lead to an increase in signal strength for the visible peak. This way, the chemical shift associated with the labelled carbon **7** can be visualised and measured, and the interconversion rate between **7** and **8** can be calculated. In a later publication by the same group this technique was expanded to other carbohydrate donors.[29] Instead of ^{13}C labels, the anomeric ^{1}H proton was used to investigate the equilibration between the α- and β triflates. Using the NMR-active ^{19}F-nucleus, exchange between the anomeric triflates and exchange with triflate species in solution was established.

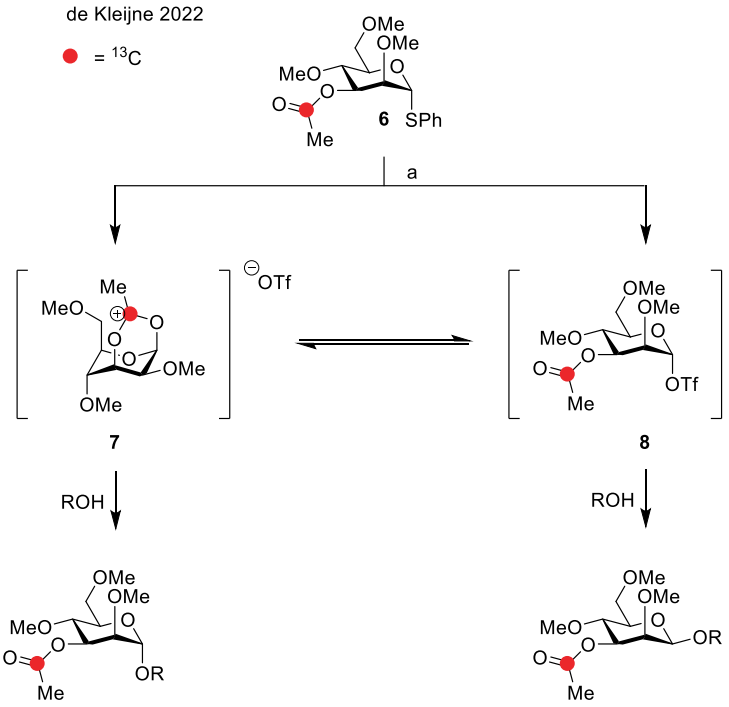

Figure 4: Structures of the mannosyl donor studied using CEST NMR.[28] Reagents and conditions: Ph_2SO, TTBP, Tf_2O, DCM-d_2, -80 °C.

Isotope Labelling without NMR

In the previous section, examples were given where isotope labelling was combined with NMR spectroscopy to gain insight into the structure and reactivity of carbohydrates. There are also numerous examples of isotopic labelling in which NMR spectroscopy is not required. For example, Egsgaard and co-workers used fully ^{13}C labelled monosaccharides as an internal standard for GC-MS experiments.[30] To investigate which monomers were present in various hemicelluloses, the hemicelluloses were hydrolysed to a mixture of monosaccharides, which was then analysed using GC-MS. Since labelled and unlabelled monosaccharides have the same retention time, but differ in molecular weight, the ^{13}C labelled monosaccharides served as the perfect internal standard. Świderski and Temeriusz used radioactive labelling techniques to investigate how sensitive methyl D-glycopyranosides are to methanolysis.[31] In their experiment, which is depicted in Figure 5, the methyl glycosides were dissolved in ^{14}C labelled methanol with 1% HCl. After the reaction, the products were crystallized and combusted, and the radioactivity of the combustion gasses was measured. The sensitivity of the substrate towards methanolysis could be measured as a function of the total amount of radioactivity. This way, it was found that α-glucose and α-mannose were relatively unreactive towards methanol under these conditions, whereas the corresponding β-glucose, β-mannose and both anomers of galactose were reactive.

Świderski and Temeriusz 1966

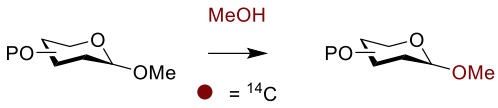

Figure 5: ^{14}C labelling experiment to investigate the activity of methyl glycopyranosides to methanolysis.[31]

Another example of a mechanistic study using labelling experiments is depicted in Figure 6.[32] Garcia and Gin developed the dehydrative glycosylation reaction depicted at the top of this figure. Here, a glycoside donor with a free hydroxyl group at the anomeric position is activated by the addition of Ph_2SO and Tf_2O. Two possible reaction mechanisms can be envisaged for this reaction: either the anomeric alcohol attacks the diphenyl sulphoxide fragment, leading to sulphoxonium ion **9**, which is in turn attacked by the nucleophile, or the anomeric alcohol attacks the triflate, leading to anomeric triflate **10**. To investigate which of these mechanisms takes place, the anomeric alcohol was labelled with an ^{18}O isotope. If the reaction takes place via the top mechanism (via **9**), the labelled oxygen atom would end up in the Ph_2SO side product, whereas the bottom mechanism, going via triflate **10**, yields ^{18}O labelled triflic acid as the by-product. After analysis of the reaction products with mass spectrometry, a 50% ^{18}O enriched Ph_2SO was found. Since two equivalents of Ph_2SO were used in the reaction, this confirms that an attack on the Ph_2SO sulphur atom takes place, and the reaction thus proceeds via intermediate **9**.

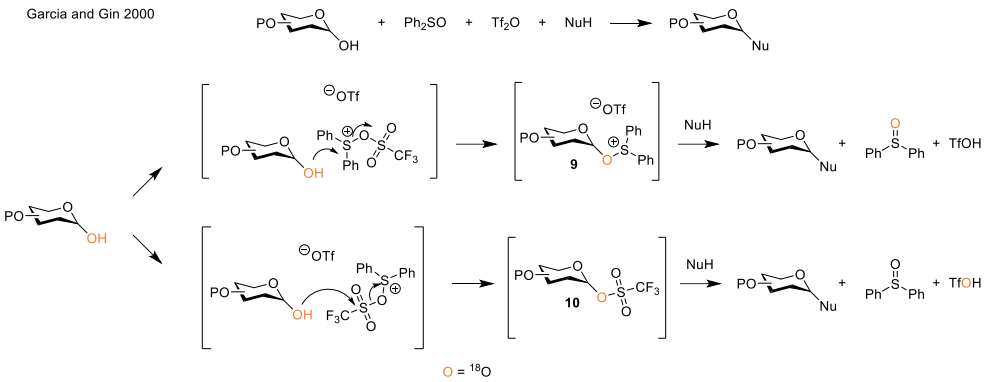

Figure 6: Investigation of the mechanism of dehydrative glycosylation via ^{18}O labelling.[32]

Isotope labels are not only visible via mass spectroscopy or, in case of NMR active isotopes, NMR spectroscopy. Replacing an atom with a heavier isotope of the same element also affects the vibrational modes of the atom, leading to small changes in the IR spectrum.[33,34] For example, a shift of around 40-43 cm^{-1} is commonly observed when comparing the vibrations of a $^{12}C=O$ to a $^{13}C=O$. This phenomenon was successfully exploited by Remmerswaal, Houthuijs *et al*. when investigating the cations formed upon activation of donor **11** in Figure 7.[35] They found that introducing the DMNPA protecting group on the C-6 position of a glucoside donor leads to a significant increase in α-selectivity of the donor. Five possible reactive cationic intermediates (structures **12a-e** in Figure 7) were investigated by DFT calculations and a combined MS-IR system to establish which species was formed in the reaction. Donor **11** was activated in the mass spectrometer, leading to the formation of a cation of which the IR spectrum was then measured and compared to the spectra calculated for **12a-e**. The calculated spectrum of cation **12c** matched best with the experimentally obtained spectrum, but a minor C=O stretch vibration was also found, which is not present in **12c**. ^{13}C Labelled donor **11** was synthesised and the IR absorption of the formed cation was measured and compared to the calculated value, which both showed a shift for an aldehyde C=O vibration. The use of the isotope-labelled donor thus confirmed that cation **12a** was also present under the activation conditions. These ring-opened structures are more often encountered when glycosyl donors are ionized in the gas phase, but they do not play a role in solution phase experiments, under normal glycosylation conditions.

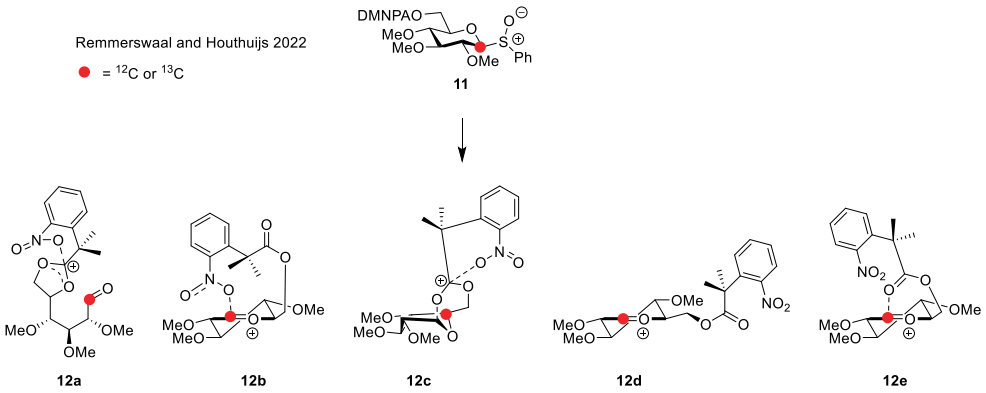

Figure 7: Possible isomers of the cation formed upon activation of **11**.[35]

Kinetic Isotope Effects (KIEs)

Isotope labelling can be used to explore reaction mechanisms by the establishment of KIEs. A KIE is defined as the ratio between the rate constant of a chemical reaction using a light isotope, k_l, and the corresponding heavy isotope, k_h (see Equation 1).[36] A KIE originates from the lowering of the zero-point energy (ZPE) as a result of exchanging an atom with a heavier isotope of the same element. The ZPE is the lowest vibrational energy (Equation 2) where n = 0, thus the ZPE is defined as ½ hν, with h being Planck's constant and ν the vibrational frequency. The frequency, in turn, is defined according to Equation 3, and depends on the force constant k, a measure of the strength of the chemical bond, and the reduced mass m_r. The reduced mass is defined by Equation 4 as the ratio between the product and the sum of the two masses on each end of the chemical bond (see Figure 8). By replacing one of these masses with a heavier isotope of the same element, the value of m_r will increase, decreasing the value of ν and the ZPE, thus stabilising the chemical bond and slightly changing the reaction kinetics. This gives rise to two types of KIE: primary KIEs, where the heavier isotope is directly involved in the chemical bond being broken and formed during the reaction, and secondary KIEs, where the heavier isotope is bound to or close to the reactive centre, but not itself involved in the bond being formed or broken.

Eq. 1: $KIE = \frac{k_l}{k_h}$

Eq. 2: $E = (n + \frac{1}{2})\, h\nu, where\ n = 0,1,2 \ldots$

Eq. 3: $\nu = \frac{1}{2\pi}\sqrt{\frac{k}{m_r}}$

Eq. 4: $m_r = \frac{m_1 m_2}{m_1 + m_2}$

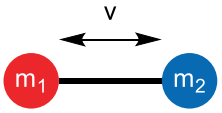

Figure 8: Schematic representation of a molecular vibration.

Primary KIEs are the direct result of lowering the ZPE. By lowering the ground state (ZPE) of a system, the energy barrier from starting materials to products is increased. For this reason, heavier isotopes generally react slower than lighter isotopes.[36] Secondary KIEs originate from the rehybridization of molecular orbitals during a chemical reaction. Going from sp^3 to sp^2 hybridisation significantly changes the vibrational modes of the system. Lowering the ZPE by changing one of the substituents for a heavier isotope thus leads to small but significant KIEs, the value of secondary KIEs being lower than for primary. For both KIEs, the numerical value depends on the reaction mechanism, with primary KIEs generally having higher values for S_N2-like reactions and secondary KIEs having higher values for S_N1-type substitutions. Both primary and secondary KIEs have been used to study a variety of mechanisms in carbohydrate chemistry, some of which will be discussed in the following section.

One of the earliest studies, investigating KIEs in carbohydrate reactivity is the hydrolysis depicted in Figure 9, reported by Sinnott and co-workers.[37] The hydrolysis of the arabinofuranoside **13** to give arabinose **14** can take place via exocyclic protonation and expulsion of the aglycon (Figure 9, mechanism **I**), or through endocyclic protonation, ring opening, hydrolysis of the oxonium ion and ring closure (mechanism **II**). To investigate the mechanism of the reaction, primary ^{18}O KIEs were used by labelling the anomeric oxygen atom. The value of the KIE was found to depend on the substituent at the anomeric position: for R = iPr, a KIE of 0.979 was found, and for R = *para*-nitrophenyl a KIE of 1.023. The diverging values provided an indication that *p*NO_2PhOH is eliminated via mechanism **I**. The hydrolysis of the *iso*-propyl arabinoside was also studied using ^2H KIE, establishing a value of 0.988, leading to the conclusion that hydrolysis of the *i*PrOH takes place via mechanism **II**. The same group used primary ^{18}O, with the ^{18}O label being present at the anomeric aglycon position, and secondary ^2H KIEs, both on the H-1 and H-2 position, to probe the enzymatic mechanism of an α-glucosidase.[38] Since no ^{18}O KIE was observed, it was concluded that breaking the anomeric C-O bond was not the rate-determining step in this reaction. Another KIE study to elucidate enzymatic reactions was described by Lee *et al*., on trehalose-6-phosphate synthase, which is a retaining glycosyltransferase enzyme.[39] Measuring the KIEs by using glucose-UDP labelled with ^2H, ^3H, ^{14}C and ^{18}O confirmed that an oxocarbenium-like transition state was present.

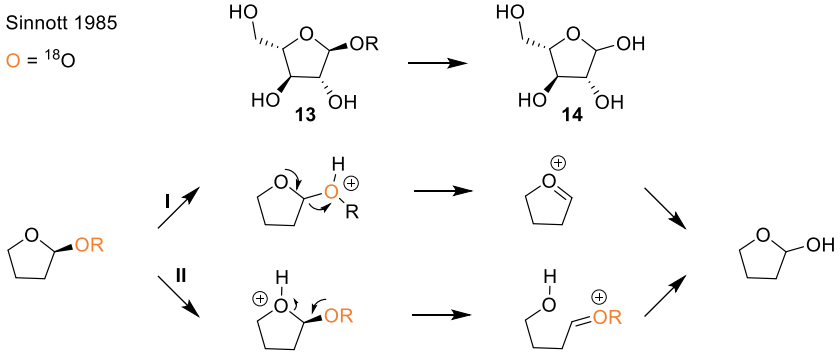

Figure 9: Mechanism of hydrolysis of arabinose using ^{18}O and ^2H KIEs.[37]

Figure 10 shows an example where a ^{2}H KIE was used to investigate the anomerisation of **15**.[40] Berven *et al*. postulated four possible mechanisms for this reaction (mechanisms **I-IV**). They found a value of 1.09 for the ^{2}H KIE of the anomeric hydrogen, which was too low for a primary KIE, but in range of a secondary KIE. Using this information, mechanism **I** was excluded, as direct proton abstraction would lead to a primary ^{2}H KIE. Using additional kinetic experiments, mechanism **IV** was revealed to be the actual mechanism.

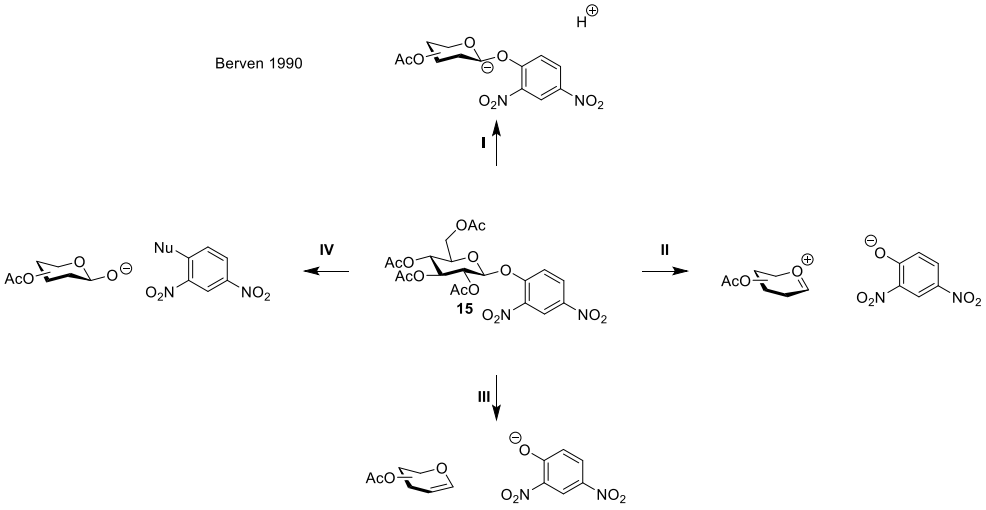

Figure 10: Possible mechanisms investigated by ^{2}H KIE.[40]

A group of glycosylation reactions that received much attention recently is the β-mannosylations. As discussed above, there are no general methodologies for the formation of *cis*-glycosidic bonds.[11–13] In 1996, however, Crich and co-workers found that when 4,6-O-benzylidene-protected mannose donors (such as **16** and **19**, Figure 11) are used, mainly β (*cis*) products are formed. [41,42] To unravel the mechanism behind this selectivity, many studies have been conducted, including the establishment of KIEs as shown in Figure 11.[12,43,44] In all three of these studies, in which both secondary ^{2}H KIEs and primary ^{13}C KIEs were established, values were found in between the values normally associated with pure S_N1 or S_N2 reactions. Using the relationship between the KIE and the structure of the transition state[45] it was concluded that the reactions in Figure 11 proceed via loosely associated transition states, which is an S_N2-like reaction mechanism, with significant charge buildup on the reactive carbon atom. [12,43,44]

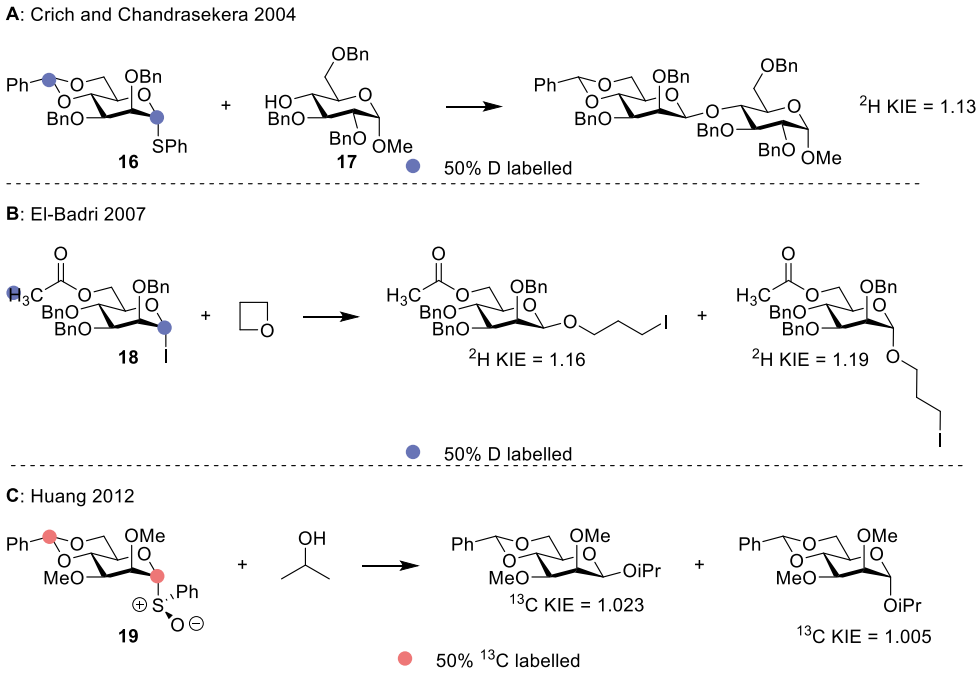

Figure 11: KIE experiments on β-mannosylation reactions.[12,43,44]

Another class of glycosylation donors that has received much attention is the benzylidene-protected glucose donor (**20** and **21**, Figure 12).[13,15] The stereoselectivity of the glycosylation reactions of these donors is highly dependent on the chosen acceptor. The KIE experiments depicted in Figure 12 were performed on this class of donors. In the study by Huang *et al.* in the glycosylation with *iso*-propanol as an acceptor (Figure 12A), KIE values were found that are neither in the S_N1, nor the S_N2 range.[44] This led to the same conclusion as for their mannose experiments described above (Figure 11C), namely that the reaction takes place via a loosely associated mechanism. Satana *et al*. (Figure 12B) used a more electron-poor acceptor, finding a relatively low (more S_N1-like) KIE.[46] From this they concluded that the reactivity of donor **21** shifts from S_N2 to S_N1 with decreasing acceptor nucleophilicity, in line with earlier mechanistic work by van der Vorm *et al*.[15,47]

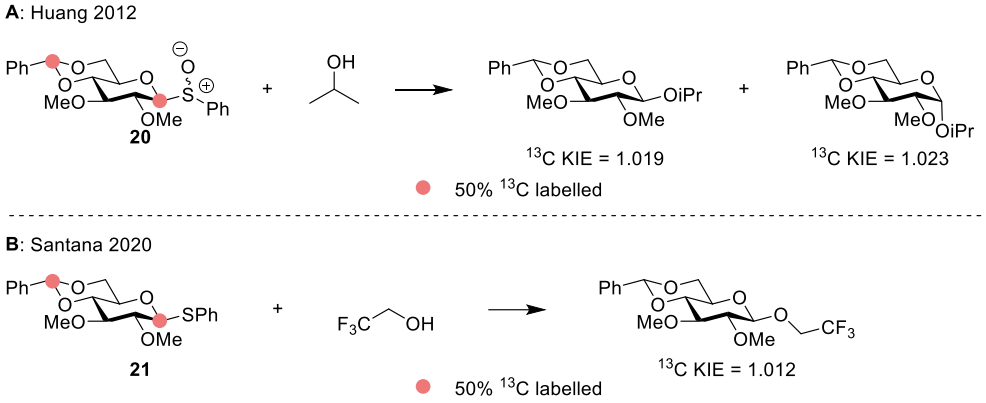

Figure 12: KIE studies on glucosylation reactions.[44,46]

Chan *et al.* performed an extensive KIE study to probe the substitution of glucosyl fluoride **22**, as shown in Figure 13.[48–50] They investigated the reactivity of this donor using different acceptors. The transition states were found by using a combination of DFT calculations and ^{2}H, ^{13}C and ^{18}O KIEs. For both HFIP[48] (Figure 13A) and the hydronium[49] (Figure 13B), where retention of anomeric configuration was observed in the reaction product, an S_Ni or front-side S_N2 mechanism was found. In the transition states of these reactions, a hydrogen bond is formed between the incoming nucleophile and the fluorine leaving group. When the azide was used as a nucleophile (Figure 13C), inversion of the anomeric stereochemistry was observed.[50] The transition state of this reaction was found to be an exploded S_N2-like transition state, similar to reactions described by Huang *et al.* (Figure 12A).[44,50]

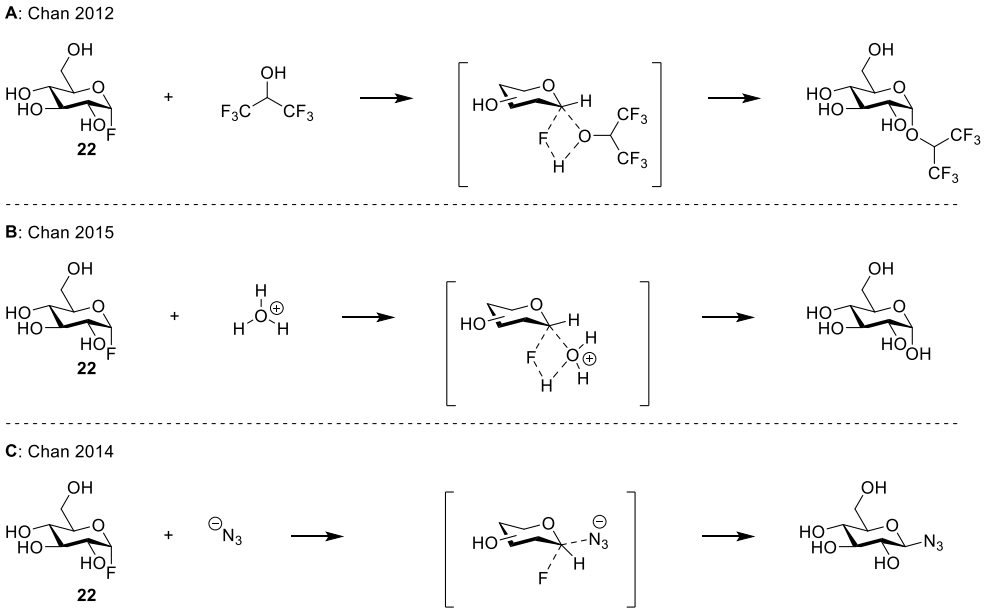

Figure 13: Transition states of the reactions of α-D-glucopyranosyl fluoride (**22**) found using ^{2}H, ^{13}C and ^{18}O KIEs.[48–50]

Overview of the Thesis

As has become clear in the preceding sections of this chapter, isotopic labelling can be used in numerous ways to better understand the structure and reactivity of carbohydrates. The research described in this thesis is used to gain further insight into different glycosylation reaction mechanisms using various systematic investigations. In chapter 2, a combination of ^{13}C and ^{15}N-labelled glycosyl trichloroacetimidate crossover experiments were used to probe the mechanism underlying the rearrangement of trichloroacetimidate glycosyl donors into the corresponding anomeric trichloroacetamides. This reaction is often described as an intramolecular rearrangement, but the crossover experiments performed in this chapter unambiguously confirm an intermolecular aglycon transfer mechanism to leads to the formation of the trichloroacetamide products. In chapter 3, a systematic investigation into the glycosylation reaction of 4,6-O-benzylidene-protected glucose donors is conducted. Both secondary ^{2}H and primary ^{13}C KIEs are measured for a set of glycosylation reactions using a series of acceptors of stepwise decreasing nucleophilicity. The established KIEs show that the β-products are formed via S_N2-type substitution of the α triflate, while for the formation of the α-products a shift in reaction mechanisms, from an S_N2 attack on the β triflate, to an S_N1-type attack on an oxocarbenium ion-like intermediate was found with decreasing acceptor nucleophilicity. These same systematic KIE experiments are performed on 4,6-O-benzylidene protected mannose donors in chapter 4. Here, no shift in the reaction mechanism with decreasing acceptor reactivity was found. Instead, for all acceptors, the reaction takes place via an exploded transition state, which explains the stable β-selectivity

observed with the range of different acceptors. Chapter 5 describes a series of competition experiments between two acceptors in a glycosylation reaction. These experiments are performed with two different galactose donor systems, a 4,6-silylene-protected donor, which gives α selective reactions, and a 2,3,4,6-benzoyl-protected donor, which is β selective. The former reacts faster with the least electron-rich acceptors, whereas the latter reacts faster with the most electron-rich acceptors. To further probe the reaction mechanism of the silylene-protected donor, it was activated using an activator with a non-coordinating BAr^F counter ion, and it was revealed that under these conditions the donor reacted faster with the most electron-rich donor. These results do not align with the standard S_N1 or S_N2 paradigm, and therefore a third mechanism, the front-face S_N2, is forwarded to play a key role in these -and possibly many other- glycosylation reactions.

References

1. Hölemann, A.; Seeberger, P. H. Carbohydrate Diversity: Synthesis of Glycoconjugates and Complex Carbohydrates. *Curr Opin Biotechnol* **2004**, *15* (6), 615–622. https://doi.org/10.1016/j.copbio.2004.10.001.
2. Sharon, N.; Lis, H. Carbohydrates in Cell Recognition. *Sci Am* **1993**, *268* (1), 82–89. https://doi.org/10.2307/24941340.
3. Cheng, T. Y.; Lin, Y. J.; Saburi, W.; Vieths, S.; Scheurer, S.; Schülke, S.; Toda, M. β-(1→4)-Mannobiose Acts as an Immunostimulatory Molecule in Murine Dendritic Cells by Binding the TLR4/MD-2 Complex. *Cells* **2021**, *10* (7). https://doi.org/10.3390/cells10071774.
4. Smith, H. A.; Gonzalez, J. T.; Thompson, D.; Betts, J. A. Dietary Carbohydrates, Components of Energy Balance, and Associated Health Outcomes. *Nutr Rev* **2017**, *75* (10), 783–797. https://doi.org/10.1093/nutrit/nux045.
5. Anish, C.; Schumann, B.; Pereira, C. L.; Seeberger, P. H. Chemical Biology Approaches to Designing Defined Carbohydrate Vaccines. *Chem Biol* **2014**, *21* (1), 38–50. https://doi.org/10.1016/j.chembiol.2014.01.002.
6. Kilcoyne, M.; Joshi, L. Carbohydrates in Therapeutics. *Cardiovasc Hematol Agents Med Chem* **2007**, *5* (3), 186–197. https://doi.org/10.2174/187152507781058663.
7. Maschauer, S.; Pischetsrieder, M.; Kuwert, T.; Prante, O. Utility of 1,3,4,6-Tetra-O-Acetyl-2-Deoxy-2-[18F] Fluoroglucopyranoside for No-Carrier-Added18F-Glycosylation of Amino Acids. *J Labelled Comp Radiopharm* **2005**, *48* (10), 701–719. https://doi.org/10.1002/jlcr.963.
8. Lepenies, B.; Yin, J.; Seeberger, P. H. Applications of Synthetic Carbohydrates to Chemical Biology. *Curr Opin Chem Biol* **2010**, *14* (3), 404–411. https://doi.org/10.1016/j.cbpa.2010.02.016.
9. Moss, G. P. BASIC TERMINOLOGY OF STEREOCHEMISTRY. *Pure Appl Chem* **1996**, *68* (12), 1979–1987. https://doi.org/10.1351/pac199668122193.
10. Goodman, L. NEIGHBORING-GROUP PARTICIPATION IN SUGARS. *Adv Carbohydr Chem* **1967**, *22*, 109–175. https://doi.org/10.1016/S0096-5332(08)60152-6.
11. Ishiwata, A.; Tanaka, K.; Ao, J.; Ding, F.; Ito, Y. Recent Advances in Stereoselective 1,2-Cis-O-Glycosylations. *Front Chem* **2022**, *10*, 5–9. https://doi.org/10.3389/fchem.2022.972429.
12. El-Badri, M. H.; Willenbring, D.; Tantillo, D. J.; Gervay-Hague, J. Mechanistic Studies on the Stereoselective Formation of β-Mannosides from Mannosyl Iodides Using α-Deuterium Kinetic Isotope Effects. *J Org Chem* **2007**, *72* (13), 4663–4672. https://doi.org/10.1021/jo070229y.
13. Chang, C.-W.; Greis, K.; Prabhu, G. R. D.; Wehner, D.; Kirschbaum, C.; Ober, K.; Torres-Boy, A. Y.; Leichnitz, S.; Meijer, G.; von Helden, G.; Seeberger, P. H.; Pagel, K. Mechanistic Insight into Benzylidene-Directed Glycosylation Reactions Using Cryogenic Infrared Spectroscopy. *Nature Synthesis* **2024**. https://doi.org/10.1038/s44160-024-00619-0.
14. Adero, P. O.; Amarasekara, H.; Wen, P.; Bohé, L.; Crich, D. The Experimental Evidence in Support of Glycosylation Mechanisms at the SN1-SN2 Interface. *Chem Rev* **2018**, *118* (17), 8242–8284. https://doi.org/10.1021/acs.chemrev.8b00083.
15. Van der Vorm, S.; Hansen, T.; Overkleeft, H. S.; Van der Marel, G. A.; Codée, J. D. C. The Influence of Acceptor Nucleophilicity on the Glycosylation Reaction Mechanism. *Chem Sci* **2017**, *8* (3), 1867–1875. https://doi.org/10.1039/c6sc04638j.
16. Dorst, K. M.; Engström, O.; Angles d'Ortoli, T.; Mobarak, H.; Ebrahemi, A.; Fagerberg, U.; Whitfield, D. M.; Widmalm, G. On the Influence of Solvent on the Stereoselectivity of Glycosylation Reactions. *Carbohydr Res* **2024**, *535*. https://doi.org/10.1016/j.carres.2023.109010.
17. Tuck, O. T.; Sletten, E. T.; Danglad-Flores, J.; Seeberger, P. H. Towards a Systematic Understanding of the Influence of Temperature on Glycosylation Reactions. *Angew Chem Int Ed* **2022**, *61* (15). https://doi.org/10.1002/anie.202115433.

18. Wang, C. C.; Chang, C. W.; Lin, M. H.; Wu, C. H.; Chiang, T. Y. Mapping Mechanisms in Glycosylation Reactions with Donor Reactivity: Avoiding Generation of Side Products. *J Org Chem* **2020**, *85* (24), 15945–15963. https://doi.org/10.1021/acs.joc.0c01313.
19. Li, X.; Huang, L.; Hu, X.; Huang, X. Thio-Arylglycosides with Various Aglycon Para-Substituents: A Probe for Studying Chemical Glycosylation Reactions. *Org Biomol Chem* **2009**, *7* (1), 117–127. https://doi.org/10.1039/b813048e.
20. Van Der Vorm, S.; Hansen, T.; Van Hengst, J. M. A.; Overkleeft, H. S.; Van Der Marel, G. A.; Codeé, J. D. C. Acceptor Reactivity in Glycosylation Reactions. *Chem Soc Rev* **2019**, *48* (17), 4688–4706. https://doi.org/10.1039/c8cs00369f.
21. van Hengst, J. M. A.; Hellemons, R. J. C.; Remmerswaal, W. A.; van de Vrande, K. N. A.; Hansen, T.; van der Vorm, S.; Overkleeft, H. S.; van der Marel, G. A.; Codée, J. D. C. Mapping the Effect of Configuration and Protecting Group Pattern on Glycosyl Acceptor Reactivity. *Chem Sci* **2023**, *14* (6), 1532–1542. https://doi.org/10.1039/d2sc06139b.
22. Patching, S. NMR-Active Nuclei for Biological and Biomedical Applications. *J Diagn Imaging Ther* **2016**, *3* (1), 7–48. https://doi.org/10.17229/jdit.2016-0618-021.
23. Schah-Mohammedi, P.; Shenderovich, I. G.; Detering, C.; Limbach, H. H.; Tolstoy, P. M.; Smirnov, S. N.; Denisov, G. S.; Golubev, N. S. Hydrogen/Deuterium-Isotope Effects on NMR Chemical Shifts and Symmetry of Homoconjugated Hydrogen-Bonded Ions in Polar Solution. *J Am Chem Soc* **2000**, *122* (51), 12878–12879. https://doi.org/10.1021/ja0017615.
24. Hamagami, H.; Yamaguchi, Y.; Tanaka, H. Chemical Synthesis of Residue-Selectively 13C and 2H Double-Isotope-Labeled Oligosaccharides as Chemical Probes for the NMR-Based Conformational Analysis of Oligosaccharides. *J Org Chem* **2020**, *85* (24), 16115–16127. https://doi.org/10.1021/acs.joc.0c01939.
25. Karplus, M. Contact Electron-Spin Coupling of Nuclear Magnetic Moments. *J Chem Phys* **1959**, *30* (1), 11–15. https://doi.org/10.1063/1.1729860.
26. Dessinges, A.; Castillon, S.; Olesker, A.; Thang, T. T.; Lukacs, G. Oxygen-17 NMR and Oxygen-18-Induced Isotopic Shifts in Carbon-13 NMR for the Elucidation of a Controversial Reaction Mechanism in Carbohydrate Chemistry. *J Am Chem Soc* **1984**, *106* (2), 450–451.
27. Risley, J. M.; Van Etten, R. L. An 18O Isotope Shift upon Carbon-13C NMR Spectra and Its Application to the Study of Oxygen Exchange Kinetics. *J Am Chem Soc* **1979**, *101* (1), 252–253. https://doi.org/10.1021/ja00495a059.
28. de Kleijne, F. F. J.; Elferink, H.; Moons, S. J.; White, P. B.; Boltje, T. J. Characterization of Mannosyl Dioxanium Ions in Solution Using Chemical Exchange Saturation Transfer NMR Spectroscopy. *Angew Chem Int Ed* **2022**, *61* (6), 1–5. https://doi.org/10.1002/anie.202109874.
29. de Kleijne, F. F. J.; ter Braak, F.; Piperoudis, D.; Moons, P. H.; Moons, S. J.; Elferink, H.; White, P. B.; Boltje, T. J. Detection and Characterization of Rapidly Equilibrating Glycosylation Reaction Intermediates Using Exchange NMR. *J Am Chem Soc* **2023**, *145* (48), 26190–26201. https://doi.org/10.1021/jacs.3c08709.
30. Sárossy, Z.; Plackett, D.; Egsgaard, H. Carbohydrate Analysis of Hemicelluloses by Gas Chromatography-Mass Spectrometry of Acetylated Methyl Glycosides. *Anal Bioanal Chem* **2012**, *403* (7), 1923–1930. https://doi.org/10.1007/s00216-012-6038-z.
31. Swiderski, J.; Temeriusz, A. STUDIES ON THE MECHANISM OF METHANOLYSIS OF SOME METHYL D-GLYCOPYRANOSIDES BY THE METHOD OF ISOTOPE EXCHANGE. *Carbohydr Res* **1966**, *3* (2), 225–229. https://doi.org/10.1016/S0008-6215(00)82054-6.
32. Garcia, B. A.; Gin, D. Y. Dehydrative Glycosylation with Activated Diphenyl Sulfonium Reagents. Scope, Mode of C(1)-Hemiacetal Activation, and Detection of Reactive Glycosyl Intermediates. *J Am Chem Soc* **2000**, *122* (18), 4269–4279. https://doi.org/10.1021/ja993595a.
33. Szafran, M.; Dega-Szafran, Z. A Critical Review of the Isotope Effect in IR Spectra. *J Mol Struct* **1994**, *321*, 57–77. https://doi.org/10.1016/0022-2860(93)08206-J.
34. Blume, A.; Hübner, W.; Messner, G. Fourier Transform Infrared Spectroscopy of 13C=O-Labelled Phospholipids Hydrogen Bonding to Carbonyl Groups. *Biochemistry* **1988**, *27* (21), 8239–8249.

35. Remmerswaal, W. A.; Houthuijs, K. J.; Van De Ven, R.; Elferink, H.; Hansen, T.; Berden, G.; Overkleeft, H. S.; Van Der Marel, G. A.; Rutjes, F. P. J. T.; Filippov, D. V.; Boltje, T. J.; Martens, J.; Oomens, J.; Codée, J. D. C. Stabilization of Glucosyl Dioxolenium Ions by "Dual Participation" of the 2,2-Dimethyl-2-(Ortho-Nitrophenyl)Acetyl (DMNPA) Protection Group for 1,2- Cis-Glucosylation. *J Org Chem* **2022**, *87* (14), 9139–9147. https://doi.org/10.1021/acs.joc.2c00808.
36. Anslyn, E. V.; Dougherty, D. A. *Modern Physical Organic Chemistry*; University Science Books, **2006**.
37. Bennet, A. J.; Sinnott, M. L.; Sulochana Wijesundera, W. S. L8O and Secondary 2H Kinetic Isotope Effects Confirm the Existence of Two Pathways for Acid-Catalysed Hydrolyses of a-Arabinofuranosides. *J. Chem. Soc., Perkin Trans. 2* **1985**, (8), 1233–1236. https://doi.org/10.1039/P29850001233.
38. Hosie, L.; Sinnott, M. L. Effects of Deuterium Substitution Alpha and Beta to the Reaction Centre, 18O Substitution in the Leaving Group, and Aglycone Acidity on Hydrolyses of Aryl Glucosides and Glucosyl Pyridinium Ions by Yeast Alpha-Glucosidase. *Biochem. J* **1985**, *226* (2), 437–446. https://doi.org/10.1042/bj2260437.
39. Lee, S. S.; Hong, S. Y.; Errey, J. C.; Izumi, A.; Davies, G. J.; Davis, B. G. Mechanistic Evidence for a Front-Side, SNi-Type Reaction in a Retaining Glycosyltransferase. *Nat Chem Biol* **2011**, *7* (9), 631–638. https://doi.org/10.1038/nchembio.628.
40. Berven, L. A.; Dolphin, D.; Withers, S. G. The Base-Catalysed Anomerization of Dinitrophenyl Glycosides: Evidence for a Novel Reaction Mechanism. *Can. J. Chem* **1990**, *68* (10), 1859. https://doi.org/10.1139/v90-288.
41. Crich, D.; Sun, S. Formation Of-Mannopyranosides of Primary Alcohols Using the Sulfoxide Method. *J Org Chem* **1996**, *61* (14), 4506–4507.
42. Crich, D.; Sun, S. Direct Synthesis Of-Mannopyranosides by the Sulfoxide Method. *J Org Chem* **1997**, *62* (5), 1198–1199. https://doi.org/https://doi.org/10.1021/jo962345z.
43. Crich, D.; Chandrasekera, N. S. Mechanism of 4,6-O-Benzylidene-Directed β-Mannosylation as Determined by α-Deuterium Kinetic Isotope Effects. *Angew Chem Int Ed* **2004**, *43* (40), 5386–5389. https://doi.org/10.1002/anie.200453688.
44. Huang, M.; Garrett, G. E.; Birlirakis, N.; Bohé, L.; Pratt, D. A.; Crich, D. Dissecting the Mechanisms of a Class of Chemical Glycosylation Using Primary 13C Kinetic Isotope Effects. *Nat Chem* **2012**, *4* (8), 663–667. https://doi.org/10.1038/nchem.1404.
45. Westaway, K. C. Determining Transition State Structure Using Kinetic Isotope Effects. *J Labelled Comp Radiopharm* **2007**, *50* (11–12), 989–1005. https://doi.org/10.1002/jlcr.1434.
46. Santana, A. G.; Montalvillo-Jiménez, L.; Díaz-Casado, L.; Corzana, F.; Merino, P.; Cañada, F. J.; Jiménez-Osés, G.; Jiménez-Barbero, J.; Gómez, A. M.; Asensio, J. L. Dissecting the Essential Role of Anomeric β-Triflates in Glycosylation Reactions. *J Am Chem Soc* **2020**, *142* (28), 12501–12514. https://doi.org/10.1021/jacs.0c05525.
47. van der Vorm, S.; van Hengst, J. M. A.; Bakker, M.; Overkleeft, H. S.; van der Marel, G. A.; Codée, J. D. C. Mapping the Relationship between Glycosyl Acceptor Reactivity and Glycosylation Stereoselectivity. *Angew Chem* **2018**, *130* (27), 8372–8376. https://doi.org/10.1002/ange.201802899.
48. Chan, J.; Tang, A.; Bennet, A. J. A Stepwise Solvent-Promoted S Ni Reaction of α-d-Glucopyranosyl Fluoride: Mechanistic Implications for Retaining Glycosyltransferases. *J Am Chem Soc* **2012**, *134* (2), 1212–1220. https://doi.org/10.1021/ja209339j.
49. Chan, J.; Tang, A.; Bennet, A. J. Transition-State Structure for the Hydronium Ion-Promoted Hydrolysis of Alpha-D-Glucopuranosyl Fluoride. *Can J Chem* **2015**, *93* (4).
50. Chan, J.; Sannikova, N.; Tang, A.; Bennet, A. J. Transition-State Structure for the Quintessential SN2 Reaction of a Carbohydrate: Reaction of α-Glucopyranosyl Fluoride with Azide Ion in Water. *J Am Chem Soc* **2014**, *136* (35), 12225–12228. https://doi.org/10.1021/ja506092h.